

# Repetition rate performance for frequency mixing of four simultaneous QPSK signals based on a SOA-MZI photonic sampling mixer

Hassan Termos<sup>a,b,\*</sup>, Ali Mansour,<sup>a</sup> and Abbass Nasser<sup>b</sup>

<sup>a</sup>ENSTA Bretagne, Lab STICC, Brest Cedex 9, France

<sup>b</sup>American University of Culture and Education, Faculty of Science, Beirut, Lebanon

**Abstract.** A simultaneous frequency up conversion of four intermediate frequency (IF) signals is carried out by utilizing a semiconductor optical amplifier Mach–Zehnder interferometer (SOA-MZI) in a differential configuration for radio over fiber applications. A sampling signal compelled by an optical pulse clock source produces 10-ps-width pulses at a repetition rate domain that is from 7.8 to 19.5 GHz. The four IF signals carrying quadratic phase shift keying (QPSK) data at frequencies  $f_m$  are up converted at the SOA-MZI output at mixing frequencies  $nf_{sk} \pm f_m$ , where  $k$  and  $m$  equal 1, 2, 3, and 4 and  $n$  is the harmonic rank of the sampling signal. The simulation study for simultaneous frequency up conversion relied on the SOA-MZI sampling mixer is developed to acquire the conversion gain and the error vector magnitude (EVM) in the repetition rate range. Using the virtual photonics integrated simulator, we show that incrementing the repetition rate from 7.8 to 19.5 GHz improves the competence and merit of the optical transmission system due to a better signal level and a lower aliased noise power with a higher sampling rate. Positive conversion gains were achieved at a higher mixing frequency for each channel. Concomitantly, the benefit on the conversion gain provided by augmenting the sampling frequency is 14 dB. By increasing the repetition rate, the EVM can be ameliorated up to 12% for all channels. In addition, it degrades more when the frequency channel increases over the repetition rate range. The maximum bit rate of 25 Gbit/s with a QPSK modulation meets the forward error correction limit. © The Authors. Published by SPIE under a Creative Commons Attribution 4.0 International License. Distribution or reproduction of this work in whole or in part requires full attribution of the original publication, including its DOI. [DOI: [10.1117/1.OE.60.11.116104](https://doi.org/10.1117/1.OE.60.11.116104)]

**Keyword:** all-optical sampling mixer; frequency up conversion; semiconductor optical amplifier Mach–Zehnder interferometer; quadratic phase shift modulation.

Paper 20210659 received Jun. 22, 2021; accepted for publication Oct. 19, 2021; published online Nov. 12, 2021.

## 1 Introduction

Radio over fiber (RoF) systems for the mixing function based on optical devices offer features including a weight decrease of heavy electrical cables, the use of a local oscillator (LO), and a vast bandwidth. In addition, miscellaneous techniques to implement mixed signals are analyzed to enhance the RoF system performance and minify the system cost.<sup>1–10</sup> Sampling methods become the most effective methods recently used to mend the characteristics of an optical transmission system. In a sampling mixer, the sampling signal, which is higher than the intermediate frequency (IF) for frequency up conversion, plays the function of a LO.

A semiconductor optical amplifier Mach–Zehnder interferometer (SOA-MZI), used as a sampling mixer to accomplish frequency mixing in standard and differential modes,<sup>11,12</sup> is an integrated all-optical switch. The SOA-MZI differential configuration displays preferable performance, such as a conversion gain, compared with the SOA-MZI standard configuration.<sup>11</sup> In this paper, four IF signals at different frequencies are simultaneously up converted at mixing frequencies  $nf_{sk} \pm f_m$  at the SOA-MZI output using a virtual photonics integrated (VPI) simulator for the first time, where  $n$  stands for the harmonics order,  $m$  is the IF channel index, and  $k$  is the repetition rate order. In addition, various sampling frequencies, spread from 7.8 to

\*Address all correspondence to Hassan Termos, [hassantermos@auce.edu.lb](mailto:hassantermos@auce.edu.lb)

19.5 GHz, are used to ameliorate the efficiency and quality of the RoF transmission system through a conversion gain and an error vector magnitude (EVM). The advantages of using this configuration to augment the sampling frequency are studied in our previous work.<sup>13</sup> By increasing the sampling frequency, the highest mixing frequency, which is the target frequency of the up converted signals, is related to different  $n$  of the sampling signal. For every channel, the up conversion obtained at the highest mixing frequency related to  $H_{10} = 10f_{s1}$  with  $f_{s1} = 7.8$  GHz can be also obtained with  $H_8 = 8f_{s2}$ ,  $H_6 = 6f_{s3}$ , and  $H_4 = 4f_{s4}$  with  $f_{s2} = 9.75$  GHz,  $f_{s3} = 13$  GHz, and  $f_{s4} = 19.5$  GHz, respectively. Moreover, the reduction of  $n$  needed to obtain a given frequency mixing is beneficial to the noise reduction. Hence, the signal-to-noise ratio (SNR) is enhanced by increasing the repetition rate of the optical pulse clock source.

In a previous work published in Refs. 11 and 13, we conducted an experimental study on the frequency conversion by all optical sampling based on a SOA-MZI. In this work, we built the same SOA-MZI using a VPI simulator. As a result, we have created the same setup as the experimental work to fairly compare between the experimental and simulation work. However, the fundamental novelty in this work lies in adding a sampling method in a SOA-MZI used in the VPI simulator to obtain simulation frequency up conversion, which is explained in the new principle, for four IF signals with very good performance of the optical transmission system. This work is done for the first time to the best of our knowledge. Hence, we have used the same characteristics of the SOA-MZI performed in a VPI simulator as the real device from CIP (40G-2R2-ORP).<sup>11,13</sup> The simultaneous up conversion system is used to achieve better quality and efficiency of the optical transmission system in comparison with the SOA-MZI for up conversion of a single IF signal.<sup>11,13</sup> In other words, we can demodulate the signal through the EVM with a variety of bit rates (BRs) at a higher mixing frequency compared with the experimental work. Hence, in simultaneous up conversion, four IF signals are frequency up converted at  $nf_{sk} \pm f_m$  at the SOA-MZI output. In addition, we study the impact of the mixed signal at the output of the SOA-MZI. EVM simulations at 25 Gbit/s and positive conversion gains are presented at the SOA-MZI output. The benefits of using the simultaneous frequency up conversion are a higher frequency range of up to 79 GHz with good characteristics of the optical transmission system. The simultaneous up conversion can be the most important RoF networks for a variety of applications including wireless networks, automotive radar, and telecommunications. These networks, which can merge electrical and optical signals, can benefit from low loss, low complexity, and broad bandwidth. The implementation of the simultaneous up conversion system presents important merits such as optical amplification, wider bandwidth, high conversion efficiency, and low-input optical power.

## 2 Principle of Simultaneous Up Conversion for Different Repetition Rates

To validate the proposed technique, the principle of simultaneous up conversion based on a SOA-MZI, for the first time and to the best of our knowledge, is discussed. The used SOA-MZI is used as a photonic sampling mixer, which depends on a cross phase modulation (XPM) of many input optical signals in the MZI built using SOAs as shown in Fig. 1. In addition, there are six inputs that are divided into four original data signals at the data port (DP), a sampling signal in the upper arm at the control port (CP), and a delayed sampling signal at the CP, in addition to an output signal that is a simultaneous up converted signal at the output port (OP) of the SOA-MZI.

In this architecture, the incoming data signals, which are intensity modulated by an electrical subcarrier carrying complex modulated data at IFs  $f_m$ , are launched into the two SOAs in the SOA-MZI. The sampling signal (A), corresponding to ultra-short clock pulses with a sampling frequency  $f_{s1} = 7.8$  GHz, is entered into the upper and lower arms of the MZI at the wavelength  $\lambda_s$ . However, the sampling signal at the lower port is slightly delayed compared with the one applied at the upper arm. As shown in the electrical spectrum of the sampling signals at the SOA-MZI input, the harmonics slightly decline with the frequency as well as the harmonic rank.

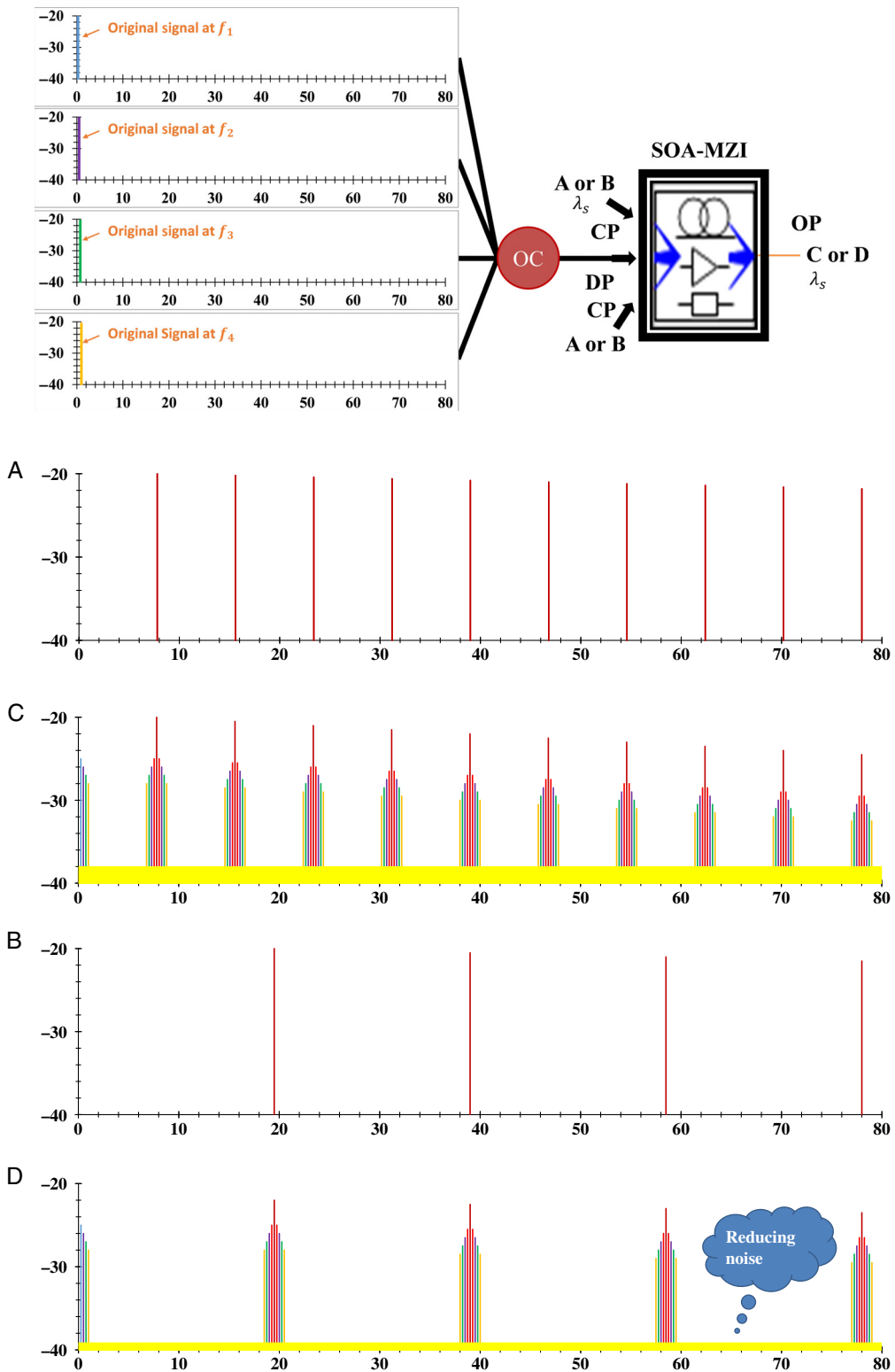


**Fig. 1** The principle of simultaneous frequency up conversion for two different sampling frequencies. (A) Sampling signal at  $f_{s1} = 7.8$  GHz, (B) sampling signal at  $f_{s4} = 19.5$  GHz, (C) simultaneous up converted signal at  $f_{s1} \pm f_m$ , and (D) simultaneous up converted at  $f_{s4} \pm f_m$ . DP, data port; CP, control port; and OP, output port.

When there is no control signal, that is the sampling signal in our case at the CP, the IF signals are amplified through two SOAs and exits at the OP of the SOA-MZI. Additionally, in the case of the presence of a sampling signal at the CP at the upper and lower arms, a phase shift is induced in the input original signals at the upper and lower output arms due to the XPM phenomenon. Thus this leads to the data signals to be sampled. As a result, the data signals are turned on and off by the sampling signal. This architecture actively turns off the SOA-MZI, which is considered to be an optical switch,<sup>14</sup> leading to a reduced transmission time window. As we can see from the electrical spectrum of the up-converted signal ( $C$ ) obtained after filtering at  $\lambda_s$ , replicas of the original data signals exist around the harmonics of the sampling signal. Replicas have different power levels depending on the harmonic rank of the sampling signal. Hence, the data signals are up converted from  $f_m$  to  $nf_{s1} \pm f_m$  at the SOA-MZI output, where  $n$  is the harmonic rank of the sampling signal. The harmonic rank ranges from 1 to 10.

This new approach is characterized by two main advantages in comparison with the previous ones demonstrated in Refs. 11 and 13. On the one hand, four IF signals are simultaneously injected at the CP of the SOA-MZI. This leads to achieving a simultaneous frequency up conversion at the SOA-MZI output. On the other hand, the optical filter after mixing is tuned at  $\lambda_s$ . This results in improving the harmonics power of the sampling signal at the higher harmonic rank. As a result, the simultaneous up converted signal has higher amplitudes at the higher mixing frequencies because its replicas follow the harmonic of the sampling signal.

However, the sampling technique has some limitations due to the bandwidth of an optical mixer and sampling noise. The bandwidth of an optical mixer limits the sampling technique, leading to increased attenuation of the harmonics as well as the replicas of the sampled signal. Another limitation of sampling is related to various noises. Thermal noise, jitter noise, beating noise, noise aliasing, and jitter noise are the rudimentary sources of noise. The spectrum contains noise merged into each Nyquist zone  $f_s/2$ . The sampled signal degrades due to the noise aliased from bands, leading to degradation of the quality of the simultaneous up conversion system. At the receiver, the photodetector generates thermal noise and shot noise in the process of moving from the optical to the electrical domain. In the presence of an amplifier, beating noise is added to the other noise.

The increase of the sampling frequency from  $f_{s1} = 7.8$  (a) to  $f_{s4} = 19.5$  GHz (b) leads to a reduction of the harmonic rank from 10 to 4, increasing the amplitude of the harmonics as well as the replica of the simultaneous up converted signal and reducing the noise as seen in (d). This leads to an improved system performance in conversion gain, EVM, and SNR. It is worth noting that we are only interested in the maximum frequency range that extends from 78.25 to 79 GHz because it is commonly used as a mixing frequency when the sampling frequency increases from 7.8 to 19.5 GHz.

### 3 Frequency Mixing Simulation Setup

A simulation setup for simultaneous all-optical frequency up conversion of RoF signals in a differential configuration is shown in Fig. 2. In this work, four IF signals (IF1, IF2, IF3, and IF4) are used to evaluate simultaneous up conversion of the optical transmission system. The IF signals are intensity modulated by an electrical subcarrier carrying quadratic phase shift keying (QPSK) data at frequencies equal to  $f_1 = 0.25$  GHz,  $f_2 = 0.5$  GHz,  $f_3 = 0.75$  GHz, and  $f_4 = 1$  GHz, respectively.

We have worked previously on the experimental study of frequency conversion by all optical sampling based on a SOA-MZI. To compare this work with a simulation one, we have bought the same SOA-MZI to be used in a VPI simulator. As a result, we have built the same setup as the experimental work.<sup>11,13</sup> The genuine SOA-MZI used in simulation by the VPI simulator is displayed in Fig. 3. This SOA-MZI performs a variety of optical logic functions and can be used in optical processing applications. It is used to obtain a frequency conversion to higher or lower frequencies by all-optical sampling, while its static and dynamic characteristics are studied to choose the best operating point used in the frequency conversion techniques. This SOA-MZI is used for the standard mode. To work in differential mode, the control signal is injected at the lower arm with a certain delay time using a variable optical delay line (VODL). As a result,

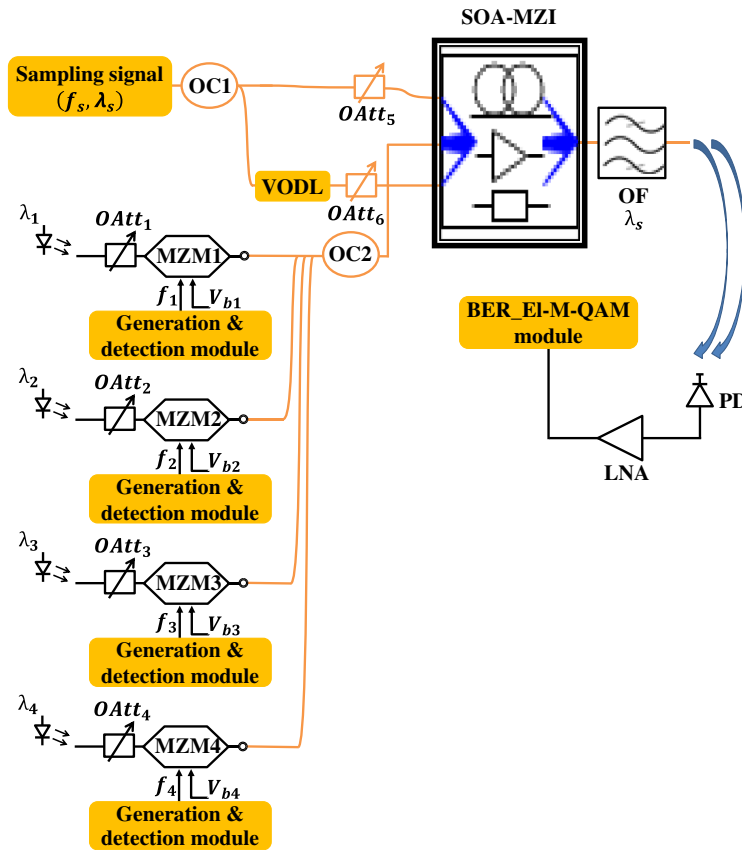


**Fig. 2** Block diagram of simulation setup of frequency mixing in a SOA-MZI differential configuration. OAtt, optical attenuator; OF, optical filter; LNA, low-noise amplifier; MZM, Mach-Zehnder modulator; PD, photodiode; BER, bit error rate; VODL, variable optical delay line; QAM, quadratic amplitude modulation; and  $V_b$ , bias voltage.

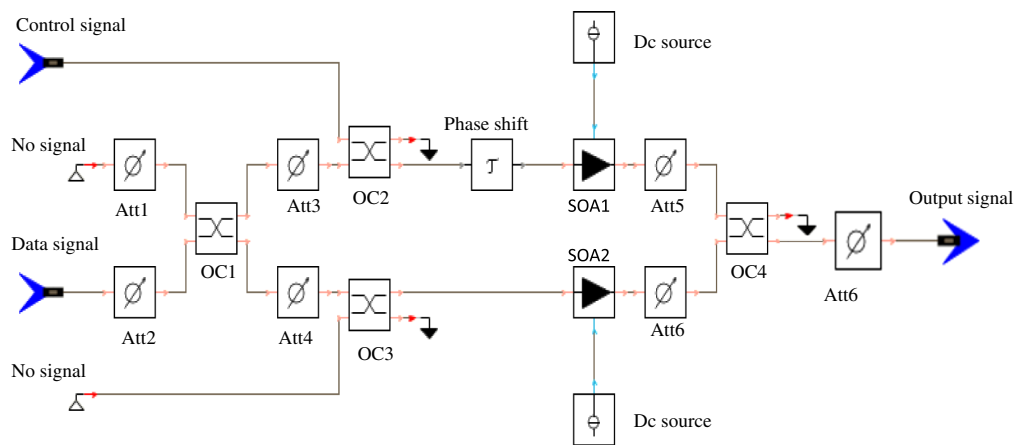


**Fig. 3** SOA-MZI schematic. Att, attenuator; OC, optical coupler; and SOA, semiconductor optical amplifier.

we have used the same SOA-MZI (structure, static, and dynamic characteristics) built in a VPI simulator as the real device from CIP (40G-2R2-ORP).<sup>11,13</sup>

The IF signals are created using laser sources, optical Mach-Zehnder modulators (MZMs), and optical attenuators (OAtt), respectively. The generation and detection module at the electrical port of the MZMs is used to produce the QPSK data. The IF data signals, which are

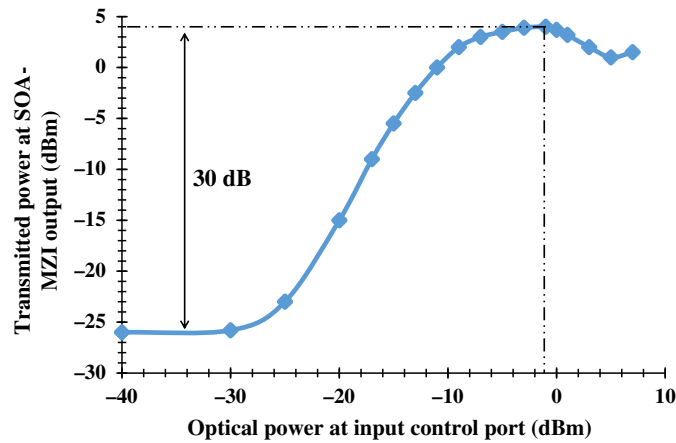


Fig. 4 Static characteristic of the SOA-MZI. The maximum ER is 30 dB.

generated by laser sources that have the same mean optical power of  $-10$  dBm at wavelengths  $\lambda_p$ , where  $p$  is an integer, are injected simultaneously into the SOA-MZI data input port. The wavelength of the data input signal spreads from  $\lambda_1 = 1445$  nm to  $\lambda_4 = 1448$  nm. The bias current of SOA1 and SOA2 is about 350 mA.

The transmitted power at the SOA-MZI output depends on the sampling signal power at  $\lambda_s = 1550$  nm, applied to the SOA-MZI control input. Figure 4 shows the SOA-MZI static characteristic with a maximum extinction ratio (ER) equal to 30 dB. According to the optical power at the control input, the maximum output power of the data input signal at the SOA-MZI output is achieved at  $-1$  dBm.

The SOA-MZI dynamic behavior depends on the carrier lifetime and the stimulated carrier recombination time.<sup>15</sup> To improve its dynamic behavior, an SOA must be biased with a high bias current, which corresponds to 350 mA for both SOAs. A mean optical power of  $-10$  dBm at  $\lambda_1 = 1545$  nm is injected at the data input, and an intensity modulated power of  $-1$  dBm at  $\lambda_s = 1550$  nm is injected at the control input. At the SOA-MZI output, the modulated data signal is photodetected and amplified. Its frequency response in Fig. 5 shows a low-pass behavior with a 7.8-GHz cutoff frequency  $f_c$ . Therefore, the repetition rate of the sampling signal is chosen to be higher than or equal to  $f_c$  to achieve better characteristics of the optical transmission system at the higher mixing frequency of up to 79 GHz, such that carrier density of the SOA is still efficaciously modulated.

The sampling signal at various repetition rates, ranging from 7.8 to 19.5 GHz, is generated by an optical pulse clock source.<sup>11-13</sup> This source provides an optical pulse train of 10 ps full-width

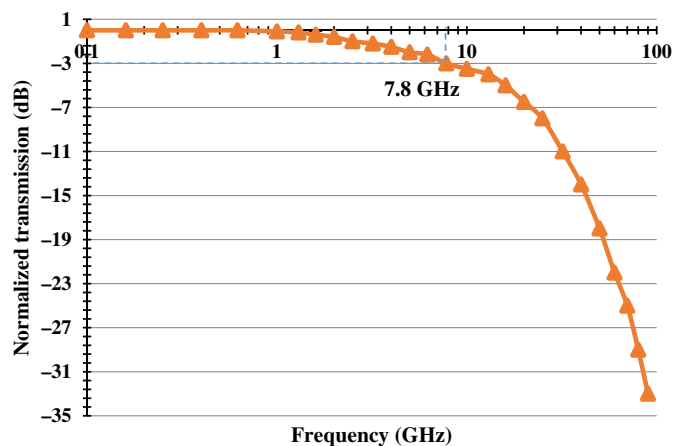


Fig. 5 SOA-MZI dynamic characteristic with the 7.8-GHz cutoff frequency.

at half-maximum pulses. Its electrical spectrum shows harmonics at  $H_n = nf_{sk}$ . To make up conversion in a differential configuration, the sampling signal is injected into both SOA-MZI input CPs. The sampling signal power at the upper and lower control inputs is, respectively,  $-1$  and  $-3$  dBm. A VODL and an OAtt are used to tune the time and power difference between pulses traveling in the upper and lower arms. The sampling signal at the lower control input is delayed by a VODL at the differential delay time of 14 ps compared with the one at the upper control arm.

At the SOA-MZI output, the wavelength of the sampling signal  $\lambda_s = 1550$  nm is used to tune an optical filter (OF). The sampled signal is photodetected with a 100-GHz photodiode (PD) having a sensitivity of 0.85 A/W, amplified by a 33-dB-gain low-noise amplifier (LNA) and displayed on an electrical spectrum analyzer (ESA) to obtain the simultaneous up conversion spectrum as well as conversion gains, or used the BER\_EL-M-QAM module to obtain the bit error rate (BER) of the sampled QPSK signal. After that, the EVM values are calculated from the measured BER. Since the sampled signal follows the harmonics of the sampling signal where its harmonics power slightly decreases at the SOA-MZI output due to the wavelength of the optical filter that is equal to the wavelength of the sampling signal,<sup>16</sup> the performance of the mixing system is enhanced sufficiently. It is worth noting that the only difference between this work and that in Ref. 16 is that the sampling signal and the data signal are exchangeable signals. In other words, the sampling signal is injected at the MP of the SOA-MZI while the data signal is entered into the CP of the SOA-MZI. However, the OF is tuned at  $\lambda_s$ .

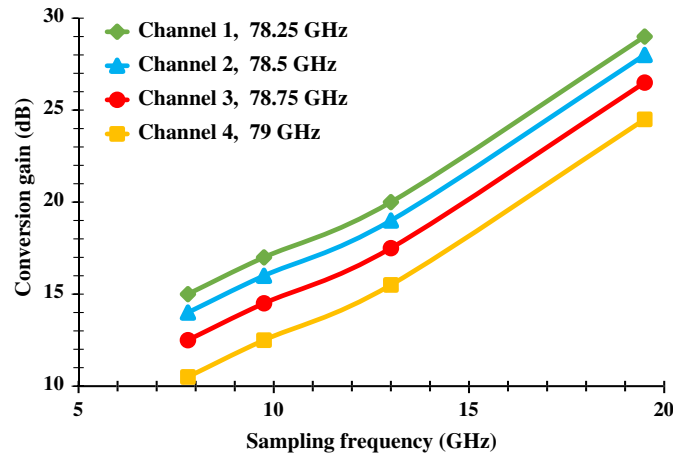
#### 4 Conversion Gain

The simulations are carried out using a VPI transmission maker.<sup>17</sup> The four optical carriers injected at the data input are intensity modulated by a sine wave signal at  $f_1 = 0.25$  GHz for the IF1 signal,  $f_2 = 0.5$  GHz for the IF2 signal,  $f_3 = 0.75$  GHz for the IF3 signal, and  $f_4 = 1$  GHz for the IF4 signal. In all cases, the mean optical power at the DP is  $-10$  dBm. The electrical power of the corresponding photodetected signal at the data input is  $-35.4$ ,  $-36.8$ ,  $-37.9$ , and  $-39$  dBm for the IF1, IF2, IF3, and IF4 signals, respectively. The sampling signal power is regulated to be  $-1$  dBm at the upper CP and  $-3$  dBm at the lower one.

The sampled signal at the SOA-MZI output is optically filtered at  $\lambda_s$  before being photodetected, amplified, and displayed on an ESA. In addition, the sampling signal has harmonics powers that slightly decrease with harmonic rank when the optical filter is regulated at  $\lambda_s$ . For each of the sampling frequencies, the four IF signals at  $f_m$  at the SOA-MZI data input were simultaneously up converted at mixing frequencies  $nf_{sk} \pm f_m$  at the SOA-MZI output. In this work, we are only interested in the highest mixing frequency of the mixed signal at the SOA-MZI output. This frequency is common when the sampling frequency is changed at the SOA-MZI control input to study the effectiveness of the optical transmission system based on the SOA-MZI sampling mixer.

To quantify the performances of the photonic sampling mixer, the conversion gain of the up converted signal is computed as the ratio of its electrical power at mixing frequencies  $nf_{sk} + f_m$  at the SOA-MZI output to one of the IF signals at  $f_m$  at the SOA-MZI input. The IF signals at  $f_m$  at the data input are up converted signals at mixing frequencies  $nf_{sk} \pm f_m$  at the SOA-MZI output, where  $k$  and  $m$  equal 1, 2, 3, and 4. The up conversion gain is only obtained at the highest mixing frequency of  $10f_{s1} + f_m$ ,  $8f_{s2} + f_m$ ,  $6f_{s3} + f_m$ , and  $4f_{s4} + f_m$  when with  $f_{s1} = 7.8$  GHz,  $f_{s2} = 9.75$  GHz,  $f_{s3} = 13$  GHz, and  $f_{s4} = 19.5$  GHz, respectively, as seen in Fig. 6. The conversion gain increases with the repetition rate, whereas it decreases with the channel. It ranges from 15 dB at  $f_{s1} = 7.8$  GHz to 29 dB at  $f_{s4} = 19.5$  GHz for channel 1. In addition, the conversion gain reaches 24.5 dB at 19.5 GHz for channel 4.

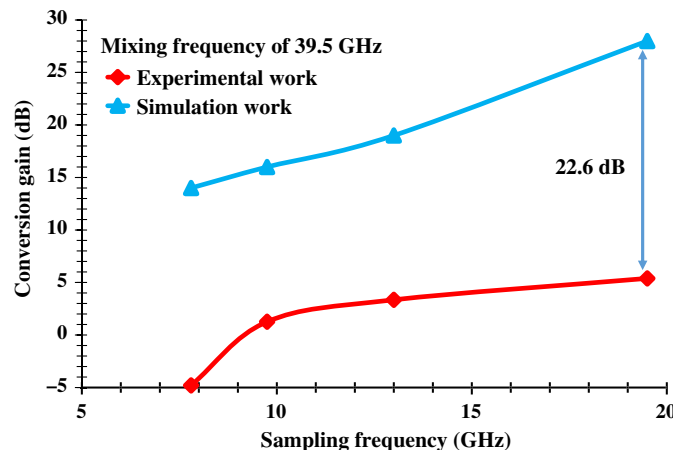
As a result, the benefit on the conversion gain provided by increasing the repetition rate from 7.8 to 19.5 GHz is about 14 dB for every channel. This is due to reducing  $n$  from 10 when  $f_{s1} = 7.8$  GHz to 4 when  $f_{s4} = 19.5$  GHz for the highest mixing frequency and improving SNR. Furthermore, positive conversion gains are obtained for the all sampling frequencies and channels at the highest mixing frequency due to increasing the sampling frequency. It is worth mentioning that the conversion gain of the sampled signal related to channel 4 degrades more than



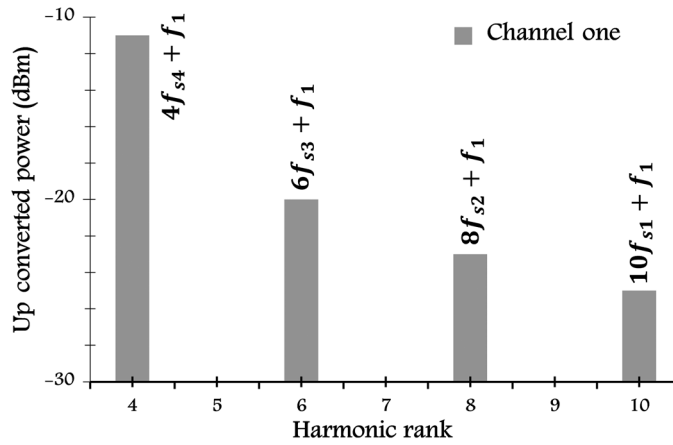
**Fig. 6** Up conversion gain at various sampling frequencies ranging from 7.8 to 19.5 GHz at the SOA-MZI output. The input IF signals at  $f_m$  are up converted at mixing frequencies  $nf_{sk} + f_m$ .

the one related to channel 1. This discrepancy is linked to various amplifications of both sub-carriers at  $f_1$  and  $f_4$  due to the SOAs: the gain difference between the low-frequency subcarrier at 0.25 GHz and the high one at 1 GHz is 10 dB. In addition, the increase of the IF frequency from 0.25 to 1 GHz leads to a decrease in the electrical power of IF signals at the SOA-MZI input and output. This results in reducing the electrical power of the up converted signal that follows the sampling signal harmonics as well as the conversion gain. Hence, the increase of the repetition rate has the same behavior of the conversion gain for every channel because it is the same sampling signal that controls the SOA-MZI, when four IF signals are up converted at the same time.

To compare with the experimental work done in Ref. 13 for different sampling frequencies, we display the conversion gain as a function of the sampling frequency at the mixing frequency of 39.5 GHz for the simulation and experimental works as seen in Fig. 7. The frequency range of 39.5 GHz is chosen because it was the maximum frequency in the experimental work. In that case, a fair comparison between them is achieved. It is worth noting that, in the experimental work, an IF signal at 0.5 GHz is only up converted at the mixing frequency of up to 39.5 GHz, which is compared with channel 2 at the same frequency in the simulation work. The conversion gain is considerably upgraded by increasing the sampling frequency for the simulation work. It reaches 28 dB at  $f_{s4} = 19.5$  GHz, which is 22.6 dB higher compared with the experimental work.



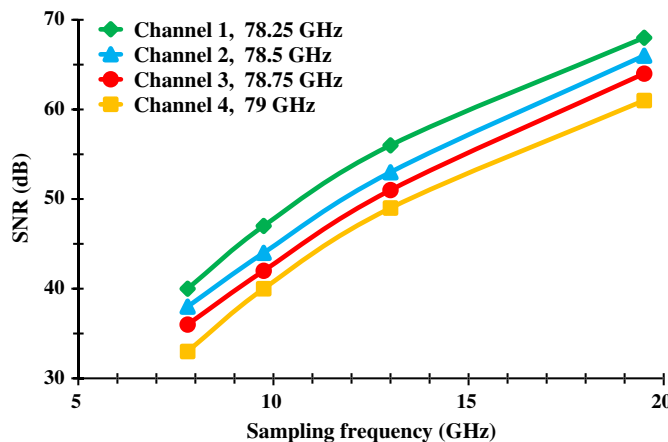
**Fig. 7** Conversion gains for simulation and experimental works at the mixing frequency of 39.5 GHz for various sampling frequencies.



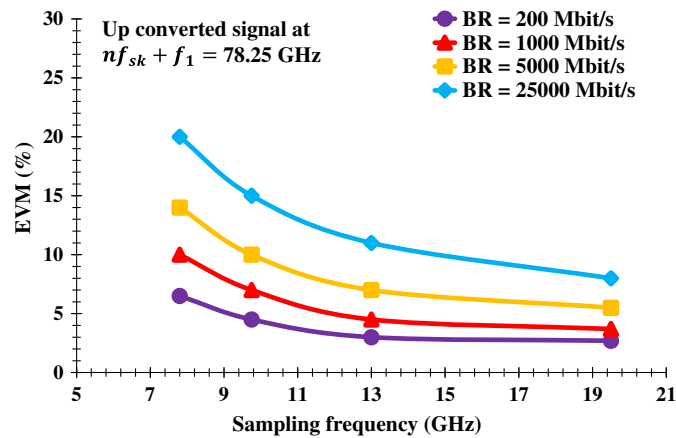
**Fig. 8** Electrical power of the up converted signal at  $nf_{sk} + f_1$  for channel 1 at the SOA-MZI output as a function of the harmonic rank for different repetition rates  $f_{sk}$ .

Figure 8 shows the up converted signal amplitude (sampled IF1 signal) at  $nf_{sk} + f_1$  at the SOA-MZI output, as a function of harmonic rank, for different repetition rates. As shown in Fig. 8, a frequency conversion obtained at  $10f_{s1} + f_1$  is obtained at  $8f_{s2} + f_1$ , leading to an increase of 2 dB of the amplitude of the up converted signal. The gain reaches up to 14 dB at  $4f_{s4} + f_1$ . In addition, the  $n$  reduction needed to obtain a given frequency shift is beneficial to the noise reduction because, in a sampled system, the periodicity of the spectrum aliases the noise power into each  $f_s/2$  Nyquist zone. The effective noise increases by the number of Nyquist zone  $n$ .<sup>18</sup> Subsequently, the SNR degradation will be reduced.

The SNR is defined as a ratio between the electrical powers of the up converted signal to the noise power. It is only obtained at the highest mixing frequency versus the sampling frequency to verify the improvement of the efficiency of the optical transmission system, see Fig. 9, for up conversion. It increases with the sampling frequency due to increasing the electrical power and decreasing the noise power of up converted signals at  $nf_{sk} + f_m$ . It ranges from 40 to 68 dB, when the repetition rate increases from 7.8 to 19.5 GHz for channel 1. The SNR is improved about 28 dB with the repetition rate for all channels. In addition, the SNR degrades about 7 dB with the channel for each sampling frequency.



**Fig. 9** SNR of up converted signals at the highest mixing frequency for different sampling frequencies and different channels.



**Fig. 10** EVM of up converted QPSK signals from  $f_1 = 0.25$  GHz to the mixing frequency  $nf_s + f_1 = 78.25$  GHz for different BRs and sampling frequencies.

### 5 Frequency Up Conversion of QPSK Data

Frequency up conversion of QPSK data carried by the electrical subcarrier at the electrical port of optical MZMs is evaluated for different BRs at the maximum mixing frequency. A generation and detection module generates QPSK data at the different carrier frequencies. The quality of the frequency mixing is evaluated through the EVM.<sup>19</sup> The EVM of the up converted signal at the SOA-MZI output was obtained through the BER\_EI-M-QAM module. As seen in Fig. 10, the EVM of up converted QPSK signals from channel 1 decreases with the repetition rate for all BRs. The EVM ranges from 6.5% at  $f_{s1} = 7.8$  GHz to 2.7% at  $f_{s4} = 19.5$  GHz at BR = 200 Mbit/s. The EVM at  $f_{s4} = 19.5$  GHz at the maximum BR = 25 Gbit/s reaches 8%. As a result, the EVM is reduced as the repetition rate increases due to the SNR improvement. Then, for a QPSK modulation, the maximum BR can attain up to 25 Gbit/s.

The EVM of sampled signals at the highest mixing frequency is also obtained for all channels at BR = 25 Gbit/s as illustrated in Fig. 11. The advantage on the EVM provided by augmenting the repetition rate from 7.8 to 19.5 GHz is 12% for all channels. In addition, the EVM degrades an average value of 7% with the channel. It increases from 8% at the mixing frequency of 78.25 GHz related to channel 1 to 15% at 79 GHz related to channel 4, at the maximum repetition rate of 19.5 GHz. It is worth noting that the transmission of the QPSK data is directly linked to the sensitivity of the receiver and not to the sensitivity of the SOA-MZI photonic mixer. The limiting factor of the receiver sensitivity, in addition to the amplification power, is the noise levels, which are reduced with the sampling frequency.

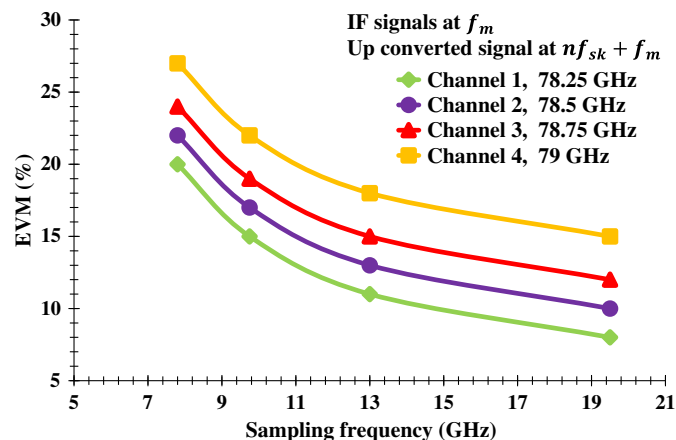


**Fig. 11** EVM of up converted QPSK signals from  $f_m$  to  $nf_{sk} + f_m$  for various sampling frequencies at BR = 25 Gbit/s.

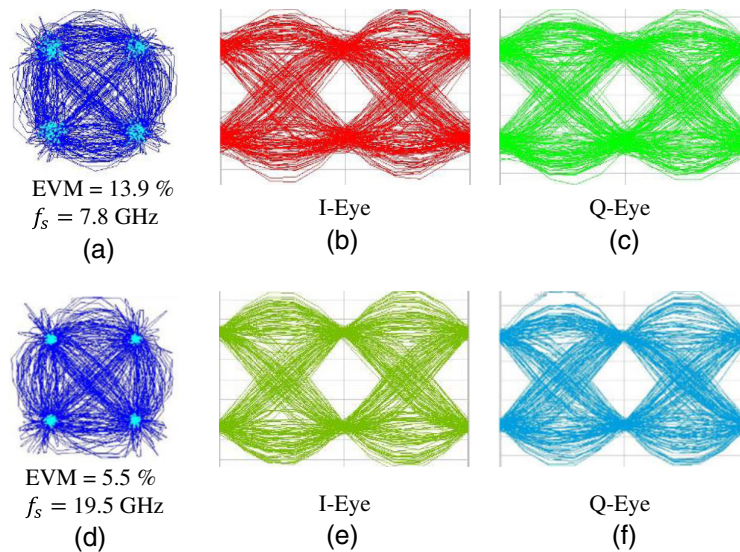


**Fig. 12** Demodulation for two QPSK up converted signals at BR = 5 Gbit/s. Constellation diagram for (a)  $f_{s1} = 7.8$  GHz and (d)  $f_{s4} = 19.5$  GHz, I-eye diagram for (b)  $f_{s1} = 7.8$  GHz and (e)  $f_{s4} = 19.5$  GHz, and Q-eye diagram for (c)  $f_{s1} = 7.8$  GHz and (f)  $f_{s4} = 19.5$  GHz.

EVM is a figure-of-merit that is related to the wireless channel networks and radar systems. During our experimental work, we used vector signal analysis (VSA) software to demodulate the mixed signal through EVM. The quality of the up converted signals can be assessed by measuring the EVM or BER. The EVM is calculated from the BER in the simulation work. In addition, it is chosen for comparison of the results with the experimental work. The relation between the BER and EVM is clearly explained in Refs. 19–21. The BER\_EL-M-QAM module of the VSA is related to the BER, and the acceptable limit is defined as the value that provides a tantamount BER of 0.0038, which secures an error free accomplishment after performing forward error correction methods.<sup>22</sup> The EVM limit for the QPSK modulation is 35%. In Fig. 11, the maximum EVM of 27% is achieved at the sampling frequency of 7.8 GHz for channel 4.

The maximum BR can attain up to 1 Gbit/s in the experiment work for the up converted signal at the mixing frequency of 39.5 GHz.<sup>13</sup> Moreover, the EVM of this signal ranges from 27.7% at the mixing frequency of 9.75 GHz to 21.2% at 19.5 GHz. When applying the simulation work, the EVM is upgraded about 17.5%. It decreases from 10 to 3.7% when the sampling frequency increases from 7.8 to 19.5 GHz at the same frequency range and BR. As a result, the simultaneous up conversion system built in the VPI simulator based on a single SOA-MZI photonic mixer for different sampling frequencies shows a clear improvement of the mixer characteristics.

The eye diagram for the in-phase-quadrature component, which visualizes the effect of noise and signal distortion as a result of transmission over a channel, can be used to assess the quality of the simultaneous up conversion system. However, we have demodulated a huge number of QPSK up converted signals at different BRs and sampling frequencies. In this case, we must display an eye diagram for each up converted signal at a specific BR or sampling frequency. Hence, we only show two constellation and eye diagrams side by side for two different sampling frequencies at BR = 5 Gbit/s as shown in Fig. 12. The significance of the increase of the sampling frequency leads to an improved EVM. This results in upgrading the constellation and eye diagrams. The eye opening corresponds to the opening in the middle, which measures the effect of noise on the signal. In (b) and (c), there is more noise, so the opening is narrower than in (e) and (f).

Single-mode fibers (SMFs) come out as the most frequently utilized transmission medium for long-distance communications. During our experimental and simulation works, we have used an SMF with a distance of up to 3 m. Hence, it ought to be affirmed that, when the simultaneous up conversion must be conveyed by a lengthy distance through an optical fiber, the dilemma of fiber chromatic distortion must be considered. A potential solution for handling the chromatic

dispersion and tackling the related problem can be achieved using a dispersion compensating fiber of a convenient length just before converting the mixed signal from the optical to electrical domains.<sup>23–26</sup> Higher noise will be unavoidable with increasing the length of real optical transmission systems, so the noise will be augmented using electrical or optical amplifiers.

## 6 Conclusion

The goal of this paper is to study the sampling rate influence in up mixing of QPSK signals using a SOA-MZI differential mode. In addition, simultaneous up conversion of four IF signals to a higher frequency range of up to 79 GHz is achieved using a VPI simulator for the first time. The obtained results show that the increase of the repetition rate, from 7.8 to 19.5 GHz, leads to a clear amelioration of the SOA-MZI performance when it is used as a sampling mixer: the signal power is improved and the aliased noise is reduced, at the same time that the  $n$  is reduced with the repetition rate. At the high sampling rate, the obtained EVM is sufficiently low to allow for BRs of up to 25 Gbit/s for all channels. Moreover, improving the harmonic power at the SOA-MZI output, especially at the higher mixing frequency, enhances the efficiency of the used sampling system.

## References

1. C. K. Sun et al., "A photonic-link millimeter-wave mixer using cascaded optical modulators and harmonic carrier generation," *IEEE Photonics Technol. Lett.* **8**(9), 1166–1168 (1996).
2. C. S. Park et al., "A photonic up-converter for a WDM radio-over-fiber system using cross-absorption modulation in an EAM," *IEEE Photonics Technol. Lett.* **17**(9), 1950–1952 (2005).
3. F. Paresys et al., "Bidirectional millimeter-wave radio-over-fiber system based on photodiode mixing and optical heterodyning," *IEEE/OSA J. Opt. Commun. Networking* **5**(1), 74–80 (2013).
4. H.-J. Song, J.S. Lee, and J.-I. Song, "Error-free simultaneous all-optical upconversion of WDM radio-over-fiber signals," *IEEE Photonics Technol. Lett.* **17**(8), 1731–1733 (2005).
5. Y.-K. Seo, C.-S. Choi, and W.-Y. Choi, "All-optical signal up-conversion for radio-on-fiber applications using cross-gain modulation in semiconductor optical amplifiers," *IEEE Photonics Technol. Lett.* **14**(10), 1448–1450 (2002).
6. H. Kim, H. Song, and J. Song, "All-optical frequency up-conversion technique using four-wave mixing in semiconductor optical amplifiers for radio-over-fiber applications," in *IEEE/MTT-S Int. Microwave Symp.*, Honolulu, pp. 67–70 (2007).
7. H.-J. Kim and J.-I. Song, "Simultaneous WDM RoF signal generation utilizing an all-optical frequency up converter based on FWM in an SOA," *IEEE Photonics Technol. Lett.* **23**(12), 828–830 (2011).
8. H.-J. Song, J. S. Lee, and J.-I. Song, "Signal up-conversion by using a cross-phase-modulation in all-optical SOA-MZI wavelength converter," *IEEE Photonics Technol. Lett.* **16**(2), 593–595 (2004).
9. J.-I. Song and H.-J. Song, "Simultaneous frequency conversion technique utilizing an SOA-MZI for full-duplex WDM radio over fiber applications," *IEICE Trans. Electron.* **E90**–C(2), 351–358 (2007).
10. N. Yan et al., "Simulation and experimental characterization of SOA-MZI-based multiwavelength conversion," *J. Lightwave Technol.* **27**(2), 117–127 (2009).
11. H. Termos et al., "All-optical radiofrequency sampling mixer based on a semiconductor optical amplifier Mach–Zehnder interferometer using a standard and a differential configuration," *J. Lightwave Technol.* **34**(20), 4688–4695 (2016).
12. D. Kastritis et al., "Modulation and switching architecture performances for frequency up-conversion of complex-modulated data signals based on a SOA-MZI photonic sampling mixer," *J. Lightwave Technol.* **38**(19), 5375–5385 (2020).
13. H. Termos, T. Rampone, and A. Sharaiha, "Sampling rate influence in up and down mixing of QPSK and OFDM signals using an SOA-MZI in a differential configuration," *Electron. Lett.* **54**(16), 990–991 (2018).

14. R. P. Schrieck et al., "All-optical switching at multi-100-Gb/s data rates with Mach-Zehnder interferometer switches," *IEEE J. Quantum Electron.* **38**(8), 1053–1061 (2002).
15. M. Spyropoulou, N. Pleros, and A. Miliou, "SOA-MZI-based nonlinear optical signal processing: a frequency domain transfer function for wavelength conversion, clock recovery, and packet envelope detection," *IEEE J. Quantum Electron.* **47**(1), 40–49 (2011).
16. H. Termos and A. Mansour, "OFDM signal down frequency conversion based on a SOA-MZI sampling mixer using differential modulation and switching architectures," *Optik* **245**, 167761 (2021).
17. VPI Transmission Maker/VPI Component Maker, version 9.4, User's Manual, Photonic Modules Reference Manuals, <https://www.vpi Photonics.com>.
18. R. G. Vaughan, N. L. Scott, and D. R. White, "The theory of bandpass sampling," *IEEE Trans. Signal Process.* **39**(9), 1973–1984 (1991).
19. R. Schmogrow et al., "Error vector magnitude as a performance measure for advanced modulation formats," *IEEE Photonics Technol. Lett.* **24**(1), 61–63 (2012).
20. M. Jeruchim, "Techniques for estimating the bit error rate in the simulation of digital communication systems," *IEEE J. Sel. Top. Quantum Electron.* **2**, 153–170 (1984).
21. R. A. Shafik, M. S. Rahman, and A. H. M. R. Islam, "On the extended relationships among EVM, BER and SNR as performance metrics," in *Proc. 4th Int. Conf. Electr. Comput. Eng.*, Dhaka, pp. 408–411 (2006).
22. M. A. Mestre et al., "Compact InP-based DFB-EAM enabling PAM-4 112 Gb/s transmission over 2 km," *J. Lightwave Technol.* **34**(7), 1572–1578 (2016).
23. B. Jopson and A. Gnauck, "Dispersion compensation for optical fiber systems," *IEEE Commun. Mag.*, **33**, 96–102 (1995).
24. X. Yi et al., "Optical device for PMD compensation by using high-birefringence linear chirped grating," in *Opt. Fiber Commun. Conf.*, pp. 315–316 (2003).
25. C. Bungarzeanu, "Limitations of dispersion supported transmission over standard single-mode fiber," *IEEE Photonics Technol. Lett.* **6**, 858–859 (1994).
26. B. Wedding, B. Franz, and B. Junginger, "10-Gb/s optical transmission up to 253 km via standard single-mode fiber using the method of dispersion-supported transmission," *J. Lightwave Technol.* **12**, 1720–1727 (1994).

**Hassan Termos** received his BS degree in physics-electronic from the Faculty of Sciences, Lebanese University, Beirut, Lebanon, in 2010. He was a master's STIP (signal processing, telecommunication, image processing and parole) student with an internship focusing on image processing at GIPSA Lab, Grenoble, France, in 2012. He received his PhD in optical communication from the Université de Bretagne Occidentale, Brest, France, in February 2017. In December 2017, he held a postdoctoral position in photonics at ENSTA Bretagne, Brest, France. He joined the American University of Culture and Education (AUCE) and Islamic University of Lebanon, Lebanon, in December 2019. His research interests are mainly in the areas of high-speed optical transmission systems and radio over fiber applications using semiconductor optical amplifiers.

**Ali Mansour** received his MS degree in electronic electric engineering from Lebanese University in September 1992, his MSc degree and PhD in signal, image, and speech processing from Instituto Politécnico Nacional de Grenoble (INPG), Grenoble, France, in July 1993 and January 1997, respectively, and his HDR degree (Habilitation à Diriger des Recherches, this is the highest of the higher degrees in the French system) from Université de Bretagne Occidentale (UBO), Brest, France, in November 2006. He held many positions such as a postdoctoral researcher at LTIRF-INPG, Grenoble, France; a researcher at RIKEN, BMC, Nagoya, Japan; a teacher-researcher position at ENSIETA, Brest, France; a senior lecturer at ECE Curtin University, Perth, Australia; an invited professor at ULCO, Calais, France; and a professor at Tabuk University, Tabuk, KSA. He is a professor at ENSTA-Bretagne, Brest, France. He published numerous refereed publications. He is the author and co-author of several books or book chapters. During his career, he successfully supervised several research associates and PhD and MSc students. He is a senior member of IEEE and was the vice president for IEEE signal processing society in Western Australia for two years. He was also the lead guest editor for

the *EURASIP Journal on Advances in Signal Processing*. He is interested in blind source separation, high-order statistics, signal processing, robotics, telecommunication, biomedical engineering, electronic warfare, and cognitive radio.

**Abbass Nasser** received his BSc degree in electronics and his MSc degree in signal, telecom, image, and speech from Lebanese University in 2010 and 2012, respectively. From 2012 to 2013, he was an assistant in the Department of Computer Science, AUCE, Lebanon. From April 2013 to December 2016, he obtained his PhD from the UBO, Brest, France. From June 2017 to May 2019, he was a postdoc researcher at ENSTA-Bretagne, Brest, France. Since June 2019, he has been an associate researcher at Ensta-Bretagne. He also has been an assistant professor at AUCE, Lebanon, since January 2017. He is participating in the supervision of several PhD projects in electronics and digital communication. He has more than 35 research papers published in international journals and conferences. His current research interests include cognitive radio, signal detection and estimation, Internet of Things, and wireless sensor networks.